REGULAR ARTICLE

FEM for elliptic eigenvalue problems: how coarse can the coarsest mesh be chosen? An experimental study

L. Banjai · S. Börm · S. Sauter

Abstract In this paper, we consider the numerical discretization of elliptic eigenvalue problems by Finite Element Methods and its solution by a multigrid method. From the general theory of finite element and multigrid methods, it is well known that the asymptotic convergence rates become visible only if the mesh width h is sufficiently small, $h \leq h_0$. We investigate the dependence of the maximal mesh width h_0 on various problem parameters such as the size of the eigenvalue and its isolation distance. In a recent paper (Sauter in Finite elements for elliptic eigenvalue problems in the preasymptotic regime. Technical Report. Math. Inst., Univ. Zürich, 2007), the dependence of h_0 on these and other parameters has been investigated theoretically. The main focus of this paper is to perform systematic experimental studies to validate the sharpness of the theoretical estimates and to get more insights in the convergence of the eigenfunctions and -values in the preasymptotic regime.

Dedicated to Wolfgang Hackbusch on the occasion of his 60th birthday.

Communicated by G. Wittum.

L. Banjai · S. Sauter (✉)
Institut für Mathematik, Universität Zürich,
Winterthurerstr 190, 8057 Zurich, Switzerland
e-mail: stas@math.unizh.ch

L. Banjai
e-mail: lehelb@math.unizh.ch

S. Börm
Institut für Informatik, Christian-Albrechts-Universität Kiel,
Christian-Albrechts-Platz 4, 24118 Kiel, Germany
e-mail: sb@informatik.uni-kiel.de

1 Introduction

The discretization of elliptic eigenvalue problems by finite elements has the same long tradition as the finite element method itself. The theory has been established, e.g., in [25], [1, Sect. 10], [2,7,8,13]. The eigenvalue multigrid method for the fast numerical solution of the arising algebraic eigenvalue problem goes back to [11]; see also [3,6,10,14–18,20,21,23, 24].

All these methods have in common that there exists a coarsest mesh width h_0 so that the asymptotic convergence estimates become visible provided $h \leq h_0$. In [22], the dependence of h_0 on the size and the isolation distance of the eigenvalue, the polynomial degree of approximation has been investigated theoretically. In this paper, we will report on some systematic numerical experiments which investigate the sharpness of the theoretical estimates for h_0 and give us more insights in the preasymptotic convergence of the eigenfunctions and -values. In [22], the focus was on the convergence of the finite element method and not on the multigrid convergence, while our numerical experiments here also address the maximal mesh width for the convergence of the eigenvalue multigrid method. In detail, we consider

1. the finite element approximation of eigenvalues,
2. the finite element approximation of the eigenvectors,
3. and the eigenvalue multigrid method.

2 Setting

Let H_0 and H_1 be real Hilbert spaces with $H_1 \subseteq H_0$ such that the embedding of H_1 in H_0 is continuous and compact. Let H'_0 and $H_{-1} := H'_1$ denote the dual spaces of H_0 and H_1. Then the embedding of H'_0 in H_{-1} is also continuous

and compact and (H_1, H_0, H_{-1}) is a Gelfand triple

$$H_1 \hookrightarrow H_0 \cong H_0' \hookrightarrow H_{-1}. \tag{2.1}$$

We denote the inner product of H_0 by $(\cdot, \cdot)_0$ and the corresponding norm by $\|\cdot\|_0$, and the inner product of H_1 by $(\cdot, \cdot)_1$ and the corresponding norm by $\|\cdot\|_1$.

The duality pairing between H_1 and H_{-1} will be denoted by $\langle \cdot, \cdot \rangle$.

Let $a : H_1 \times H_1 \to \mathbb{R}$ denote a bilinear form which satisfies the following conditions.

Assumption 2.1 The bilinear form $a : H_1 \times H_1 \to \mathbb{R}$ has the following properties.

a. Symmetry

$$a(u, v) = a(v, u) \qquad \forall u, v \in H_1.$$

b. Continuity: There exists $C_c > 0$ such that

$$|a(u, v)| \le C_c \|u\|_1 \|v\|_1 \qquad \forall u, v \in H_1.$$

c. Coercivity: There exists $\alpha > 0$ such that

$$a(u, u) \ge \alpha \|u\|_1^2 \qquad \forall u \in H_1. \tag{2.2}$$

In this paper, we will investigate the numerical computation of the following eigenvalue problem: find eigenpairs $(\lambda, e) \in \mathbb{C} \times (H_1 \setminus \{0\})$ such that

$$a(e, v) = \lambda(e, v)_0 \qquad \forall v \in H_1. \tag{2.3}$$

The spectrum, i.e., the set of all eigenvalues of (2.3), is denoted by σ and the resolvent set is defined by $\rho := \mathbb{C} \setminus \sigma$.

The *Galerkin discretization* of (2.3) is based on a finite dimensional subspace $S \subset H_1$ and is given by seeking pairs $(\lambda_S, e_S) \in \mathbb{C} \times (S \setminus \{0\})$ such that

$$a(e_S, v) = \lambda_S(e_S, v)_0 \qquad \forall v \in S. \tag{2.4}$$

The set of all discrete eigenvalues is denoted by σ_S. Although the eigenvalue problems (2.3) and (2.4) are symmetric and so all eigenvalues are real, we have complexified the problem in the usual manner in order to employ some tools from complex operator theory.

3 Multigrid method

In [11], a multigrid method has been proposed to solve elliptic eigenvalue problems efficiently. We briefly recall the method in the form of a matrix eigenvalue problem.

Let $\lambda \in \sigma$ denote the exact eigenvalue (with multiplicity $m \ge 1$) which we are going to approximate and let $\mathcal{E}(\lambda)$

denote the corresponding eigenspace. The isolation distance of λ is given by

$$\delta(\lambda) := \text{dist}(\lambda, \sigma \setminus \{\lambda\}). \tag{3.1}$$

For ease of presentation we assume that there exists a positive constant $C_{\text{gap}} < \infty$ such that

$$\sup_{\lambda \in \sigma} \frac{\delta(\lambda)}{\lambda} \le C_{\text{gap}}. \tag{3.2}$$

In [22] it was proved that—if the finite element space S satisfies a certain condition on the maximum mesh width [cf. (4.2)]—the dimension of the discrete analogue

$$\mathcal{E}_S(\lambda) := \bigoplus_{\lambda_S \in \sigma_S(\lambda)} \{u_S \in S \mid \forall v_S \in S : a(u_S, v_S) \\ = \lambda_S(u_S, v_S)_0\}, \tag{3.3}$$

has dimension m, where

$$\sigma_S(\lambda) := \sigma_S \cap B_\lambda \tag{3.4}$$

and B_λ denotes a ball in the complex plane about λ with radius

$$R := \delta(\lambda) \frac{1}{2 + 3\frac{\delta(\lambda)}{\lambda}}.$$

In order to keep the presentation simple, we restrict to the case that the geometric multiplicity of all eigenvalues $\lambda \in \sigma$ equals 1. Then (3.4) implies that $\#\sigma_S(\lambda) = m = 1$ holds, and that for $\lambda_S \in \sigma_S(\lambda)$ a vector $e_S \in S$ exists that satisfies

$$\|e_S\|_0 = 1, a(e_S, v_S) = \lambda_S(e_S, v_S)_0 \text{ for all } v_S \in S,$$

i.e., e_S is a unit-norm eigenvector for the eigenvalue λ_S of the discrete problem.

In order to use a *multigrid* method, we choose a nested hierarchy

$$S_0 \subseteq S_1 \subseteq \cdots \subseteq S_L = S \subseteq H_1$$

of subspaces of H_1. For each level $\ell \in \mathbb{N}_0$, we introduce the operators

$$A_\ell : S_\ell \to S_\ell', \quad \langle A_\ell u_\ell, v_\ell \rangle = a(u_\ell, v_\ell) \quad \text{for all } u_\ell, v_\ell \in S_\ell,$$
$$M_\ell : S_\ell \to S_\ell', \quad \langle M_\ell u_\ell, v_\ell \rangle = (u_\ell, v_\ell)_0 \quad \text{for all } u_\ell, v_\ell \in S_\ell.$$

The transfer between different levels is handled by the operator

$$P_\ell : S_{\ell-1} \to S_\ell,$$

called the *prolongation* in this context, and its dual

$$R_\ell := P_\ell^* : S_\ell' \to S_{\ell-1}',$$

which is called the *restriction*.

Using the notations

$$\lambda_\ell := \lambda_{S_\ell}, e_\ell := e_{S_\ell}$$

for the approximations of eigenvalues and eigenvectors on the different levels of the grid hierarchy, our task now is to find $\lambda_\ell \in \mathbb{R}$ and an $e_\ell \in S_\ell$ such that

$$A_\ell e_\ell = \lambda_\ell M_\ell e_\ell, \quad \langle M_\ell e_\ell, e_\ell \rangle = 1$$

holds. The eigenvalue multigrid method [11] constructs a sequence of approximate eigenvalues $\lambda_\ell^{(i)}$ and approximate eigenvectors $e_\ell^{(i)}$ by a procedure consisting of three steps: the new approximate eigenvector is constructed by performing a number of multigrid steps for computing $\tilde{e}_l^{(i+1)}$ in

$$A_\ell \tilde{e}_\ell^{(i+1)} - \lambda_\ell^{(i)} M_\ell \tilde{e}_\ell^{(i+1)} = 0. \tag{3.5}$$

The resulting vector is normalized with respect to the H_0 inner product, i.e.,

$$e_\ell^{(i+1)} := \frac{\tilde{e}_\ell^{(i+1)}}{\langle M_\ell \tilde{e}_\ell^{(i+1)}, \tilde{e}_\ell^{(i+1)} \rangle}$$

is computed, and a new approximate eigenvalue is determined by the Rayleigh quotient (the denominator can be neglected due to the normalization of $e_\ell^{(i+1)}$)

$$\lambda_\ell^{(i+1)} := \left\langle A_\ell e_\ell^{(i+1)}, e_\ell^{(i+1)} \right\rangle.$$

The main challenge is obviously the computation of the approximate solution $\tilde{e}_\ell^{(i+1)}$ of (3.5). In order to handle this task, we fix operators

$$N_\ell : S_\ell' \to S_\ell \quad \text{for all } \ell \in \{0, \ldots, L\}$$

such that $N_\ell b_\ell$ can be computed efficiently for $b_\ell \in S_\ell'$ and that N_ℓ is a reasonable approximation of A_ℓ^{-1} for oscillatory functions. A typical choice for N_ℓ is

$$N_\ell b_\ell := \theta \sum_{i \in \mathcal{I}_\ell} \frac{\langle b_\ell, \varphi_{\ell,i} \rangle}{\langle A_\ell \varphi_{\ell,i}, \varphi_{\ell,i} \rangle} \varphi_{\ell,i} \quad \text{for all } b_\ell \in S_\ell',$$

where $(\varphi_{\ell,i})_{i \in \mathcal{I}_\ell}$ is a finite-element basis of S_ℓ and $\theta \in \mathbb{R}_{>0}$ is a damping parameter. This matrix N_ℓ corresponds to the well-known damped Jacobi scheme, and it has been proven to handle oscillatory functions very well if θ is chosen correctly (cf. [12]). From the perturbation lemma [12, Criterion 6.2.7], it is easy to see that the smoothing property holds for the damped Jacobi method applied to the indefinite system $A_\ell e_\ell - \lambda_\ell M_\ell e_\ell$ under the conditions that $\lambda_\ell h_\ell^2 \to 0$ as $h_\ell \to 0$ and for some grid-independent damping parameter $\theta \lesssim 1$.

Remark 3.1 (Implementation) In an implementation, the spaces S_ℓ are represented by finite element bases $(\varphi_{\ell,i})_{i \in \mathcal{I}_\ell}$. A function $u_\ell \in S_\ell$ is described by the coefficient vector $\mathbf{u}_\ell \in \mathbb{R}^{\mathcal{I}_\ell}$ corresponding to the basis, while a functional $f_\ell \in S_\ell'$ is described by the coefficient vector $\mathbf{f}_\ell \in \mathbb{R}^{\mathcal{I}_\ell}$ corresponding to the dual basis, i.e.,

$$u_\ell = \sum_{i \in \mathcal{I}_\ell} \mathbf{u}_{\ell,i} \varphi_{\ell,i}, \quad \mathbf{f}_{\ell,j} = \langle f_\ell, \varphi_{\ell,j} \rangle \quad \text{for all } j \in \mathcal{I}_\ell.$$

The operators A_ℓ and M_ℓ map functions to functionals, therefore the straightforward representation is to use the standard stiffness and mass matrices $\mathbf{A}_\ell, \mathbf{M}_\ell \in \mathbb{R}^{\mathcal{I}_\ell \times \mathcal{I}_\ell}$ given by

$$(\mathbf{A}_\ell)_{ij} = \langle A_\ell \varphi_{\ell,j}, \varphi_{\ell,i} \rangle, \quad (\mathbf{M}_\ell)_{ij} = \langle M_\ell \varphi_{\ell,j}, \varphi_{\ell,i} \rangle,$$
$$\text{for all } i, j \in \mathcal{I}_\ell.$$

The prolongation operator P_ℓ maps functions to functions, therefore we represent it by a matrix $\mathbf{P}_\ell \in \mathbb{R}^{\mathcal{I}_\ell \times \mathcal{I}_{\ell-1}}$ satisfying

$$P_\ell \varphi_{\ell-1,j} = \sum_{i \in \mathcal{I}_\ell} (\mathbf{P}_\ell)_{ij} \varphi_{\ell,i} \quad \text{for all } j \in \mathcal{I}_{\ell-1}.$$

By the same reasoning, the smoothing operator N_ℓ corresponds to a diagonal matrix $\mathbf{N}_\ell \in \mathbb{R}^{\mathcal{I}_\ell \times \mathcal{I}_\ell}$ with

$$(\mathbf{N}_\ell)_{ij} = \begin{cases} \theta / \mathbf{A}_{ii} & \text{if } i = j, \\ 0 & \text{otherwise} \end{cases} \quad \text{for all } i, j \in \mathcal{I}_\ell.$$

Using these basis representations, applying an operator to a function or functional is equivalent to a matrix-vector multiplication, and evaluating the dual product $\langle \cdot, \cdot \rangle$ corresponds to a simple Euclidean product:

$$\langle f_\ell, u_\ell \rangle = \sum_{i \in \mathcal{I}_\ell} \mathbf{u}_{\ell,i} \langle f_\ell, \varphi_{\ell,i} \rangle = \sum_{i \in \mathcal{I}_\ell} \mathbf{u}_{\ell,i} \mathbf{f}_{\ell,i} = \mathbf{f}_\ell^\top \mathbf{u}_\ell.$$

3.1 Eigenvalue multigrid iteration

The multigrid scheme consists of three phases: first oscillatory components of the error are reduced using the *smoothing iteration*

$$\tilde{e}^{(i,0)} := e^{(i)}, \quad \tilde{e}^{(i,j+1)} := \tilde{e}^{(i,j)} - N_\ell \left(A_\ell \tilde{e}^{(i,j)} - \lambda_\ell^{(i)} M_\ell \tilde{e}^{(i,j)} \right)$$
$$\text{for all } j \in \{0, \ldots, \nu - 1\}.$$

We can assume that the remaining error is smooth enough to be approximated in a coarser space, so we compute the defect

$$d_\ell^{(i)} := A_\ell \tilde{e}^{(i,\nu)} - \lambda_\ell^{(i)} M_\ell \tilde{e}^{(i,\nu)}$$

and transfer it to the coarser space $S_{\ell-1}$ using the restriction

$$b_{\ell-1}^{(i)} := R_\ell d_\ell^{(i)}.$$

In the coarser grid, we (approximately) solve the coarse-grid equation

$$A_{\ell-1} c_{\ell-1}^{(i)} - \lambda_{\ell-1} M_{\ell-1} c_{\ell-1}^{(i)} = b_{\ell-1}^{(i)} \tag{3.6}$$

by using an appropriate *singular multigrid algorithm* and then add the correction $c_{\ell-1}^{(i)}$ to $\tilde{e}^{(i,\nu)}$ in order to get the next approximation

$$\tilde{e}_\ell^{(i+1)} := \tilde{e}_\ell^{(i,\nu)} - P_\ell c_{\ell-1}^{(i)}.$$

If necessary, we can use additional smoothing steps to eliminate oscillatory errors introduced by the prolongation and get the following algorithm:

procedure EMG(ℓ, **var** λ_ℓ, e_ℓ);
    for $i := 1$ **to** ν_1 **do**
        $e_\ell \leftarrow e_\ell - N_\ell(A_\ell e_\ell - \lambda_\ell M_\ell e_\ell)$;
    $d_\ell \leftarrow A_\ell e_\ell - \lambda_\ell M_\ell e_\ell$;
    $b_{\ell-1} \leftarrow R_\ell d_\ell$; $c_{\ell-1} \leftarrow 0$;
    for $i := 1$ **to** γ **do**
        SMG($\ell - 1, b_{\ell-1}, c_{\ell-1}$);
    $e_\ell \leftarrow e_\ell - P_\ell c_{\ell-1}$;
    for $i := 1$ **to** ν_2 **do**
        $e_\ell \leftarrow e_\ell - N_\ell(A_\ell e_\ell - \lambda_\ell M_\ell e_\ell)$;
    $e_\ell \leftarrow e_\ell / \langle M_\ell e_\ell, e_\ell \rangle$;
    $\lambda_\ell \leftarrow \langle A_\ell e_\ell, e_\ell \rangle$

In this algorithm, ν_1 and ν_2 are the numbers of the pre- and postsmoothing steps and γ is the number of recursive multigrid calls: $\gamma = 1$ corresponds to the V-cycle, $\gamma = 2$ to the W-cycle.

3.2 Singular multigrid iteration

Let us now consider the coarse-grid equation (3.6). Since $\lambda_{\ell-1}$ is an eigenvalue of $A_{\ell-1}$, we have to solve a *singular* system.

We investigate the general system

$$B_\ell x_\ell = f_\ell \qquad (3.7)$$

for an operator $B_\ell : S_\ell \to S'_\ell$, a right-hand side $f_\ell \in S'_\ell$, and the solution $x_\ell \in S_\ell$. We assume that the kernel of B_ℓ is spanned by a known vector $k_\ell \in S_\ell$ and that the range of B_ℓ is perpendicular to this vector, i.e.,

$$\text{Range}(B_\ell) = \{g_\ell \in S'_\ell \ : \ \langle g_\ell, k_\ell \rangle = 0\}.$$

In the case of the eigenvalue problem, these conditions hold for $B_\ell = A_\ell - \lambda_\ell M_\ell$ and $k_\ell = e_\ell$, since $A_\ell^{-1}(A_\ell - \lambda_\ell M_\ell)$ is a Fredholm operator and A_ℓ and M_ℓ are self-adjoint.

The system (3.7) can only be solved if $f_\ell \in \text{Range}(B_\ell)$ holds, and due to our assumption, this is equivalent to $\langle f_\ell, k_\ell \rangle = 0$. If this equation is not valid, we replace f_ℓ by the corrected right-hand side

$$\tilde{f}_\ell := f_\ell - \frac{\langle f_\ell, k_\ell \rangle}{\langle M_\ell k_\ell, k_\ell \rangle} M_\ell k_\ell \qquad (3.8)$$

and observe that the latter satisfies

$$\langle \tilde{f}_\ell, k_\ell \rangle = \langle f_\ell, k_\ell \rangle - \frac{\langle f_\ell, k_\ell \rangle}{\langle M_\ell k_\ell, k_\ell \rangle} \langle M_\ell k_\ell, k_\ell \rangle = 0,$$

therefore we have $\tilde{f}_\ell \in \text{range}(B_\ell)$ and can find a solution of the corrected system

$$B_\ell x_\ell = \tilde{f}_\ell.$$

This solution, however, is not unique: we can add arbitrary multiples of k_ℓ to x_ℓ without changing the right-hand side. In order to guarantee uniqueness, we introduce the additional condition $\langle M_\ell k_\ell, x_\ell \rangle = 0$, i.e., we require the solution to be perpendicular to the kernel of B_ℓ.

Given an arbitrary solution x_ℓ of (3.7), this condition can be fulfilled by using

$$\tilde{x}_\ell := x_\ell - \frac{\langle M_\ell k_\ell, x_\ell \rangle}{\langle M_\ell k_\ell, k_\ell \rangle} k_\ell, \qquad (3.9)$$

since this function satisfies

$$\langle M_\ell k_\ell, \tilde{x}_\ell \rangle = \langle M_\ell k_\ell, x_\ell \rangle - \frac{\langle M_\ell k_\ell, x_\ell \rangle}{\langle M_\ell k_\ell, k_\ell \rangle} \langle M_\ell k_\ell, k_\ell \rangle = 0.$$

The singular multigrid iteration consists of four main steps: the right-hand side f_ℓ is corrected to fit into range(B_ℓ), some smoothing iterations are applied, the coarse-grid problem is solved by recursive calls, and the result is corrected to ensure that it is perpendicular on k_ℓ.

In the case of the eigenvalue problem, the projections (3.8) and (3.9) can be simplified by taking advantage of the normalization $\langle M_\ell e_\ell, e_\ell \rangle = 1$, and we arrive at the following algorithm:

procedure SMG(ℓ, f_ℓ, **var** x_ℓ);
    $f_\ell \leftarrow f_\ell - \langle f_\ell, e_\ell \rangle M_\ell e_\ell$;
    if $\ell = 0$ **then**
        $x_\ell \leftarrow (A_\ell - \lambda_\ell M_\ell)^{-1} f_\ell$
    else begin
        for $i := 1$ **to** ν_1 **do**
            $x_\ell \leftarrow x_\ell - N_\ell(A_\ell x_\ell - \lambda_\ell M_\ell x_\ell - f_\ell)$;
        $d_\ell \leftarrow A_\ell x_\ell - \lambda_\ell M_\ell x_\ell - f_\ell$;
        $f_{\ell-1} \leftarrow R_\ell d_\ell$; $x_{\ell-1} \leftarrow 0$;
        for $i := 1$ **to** γ **do**
            SMG($\ell - 1, f_{\ell-1}, x_{\ell-1}$);
        $x_\ell \leftarrow x_\ell - P_\ell x_{\ell-1}$;
        for $i \leftarrow 1$ **to** ν_2 **do**
            $x_\ell \leftarrow x_\ell - N_\ell(A_\ell x_\ell - \lambda_\ell M_\ell x_\ell - f_\ell)$
    end;
    $x_\ell \leftarrow x_\ell - \langle M_\ell e_\ell, x_\ell \rangle e_\ell$

Note that the matrix $A_0 - \lambda_0 M_0$ which appears on the coarsest level of SMG is singular and cannot be inverted. In our program, we have realized the solution of the singular system $(A_0 - \lambda_0 M_0) x_0 = f_0$ by employing an LU factorization with partial pivoting (LAPACK routines dgbtrf and dgbtrs) and they do not report any errors. This is probably due to rounding errors occurring during the factorization. The resulting instability is compensated by the projections into the complement of the eigenspace.

3.3 Nested iteration

The singular multigrid iteration works only for a level ℓ if sufficiently accurate approximations of the eigenvectors $e_0, \ldots, e_\ell$ are available. This means that the eigenvalue

multigrid algorithm can only work for a level ℓ if the eigenvectors $e_0, \ldots, e_{\ell-1}$ are available.

In order to meet this requirement, we use a nested iteration (sometimes also called full multigrid) scheme:

> **procedure** EMGFull;
> Solve $A_0 e_0 = \lambda_0 M_0 e_0$;
> $e_0 \leftarrow e_0 / \langle M_0 e_0, e_0 \rangle$;
> **for** $\ell \leftarrow 1$ **to** L **do begin**
> $\quad e_\ell \leftarrow P_\ell e_{\ell-1}$;
> $\quad \lambda_\ell \leftarrow \lambda_{\ell-1}$;
> $\quad$ **for** $i \leftarrow 1$ **to** μ **do**
> $\quad\quad$ EMG$(\ell, \lambda_\ell, e_\ell)$
> **end**

We have iterated the routine EMG in EMGFull on level ℓ always up to convergence by choosing the parameter μ appropriately.

It is important to note that the Galerkin property implies

$$\langle M_\ell P_\ell e_{\ell-1}, P_\ell e_{\ell-1} \rangle = \langle M_{\ell-1} e_{\ell-1}, e_{\ell-1} \rangle,$$
$$\langle A_\ell P_\ell e_{\ell-1}, P_\ell e_{\ell-1} \rangle = \langle A_{\ell-1} e_{\ell-1}, e_{\ell-1} \rangle,$$

therefore the function $P_\ell e_{\ell-1}$ will be normalized, and its Rayleigh quotient will be equal to the coarse-grid eigenvalue $\lambda_{\ell-1}$.

In addition to ensuring that the singular multigrid algorithm SMG is applicable, the nested iteration also provides us with very good initial guesses for the eigenvectors and eigenvalues, therefore we can expect that a small number of EMG steps will be sufficient to compute good approximations.

If the dimensions of the spaces S_ℓ decay exponentially, i.e., if dim $S_\ell > q$ dim $S_{\ell-1}$ holds for all $\ell \in \{1, \ldots, L\}$ with a factor $q > 1$, the complexity of the entire nested iteration scheme EMGFull is dominated by the highest level L, so using a simple smoother like Jacobi yields an algorithm of linear complexity. This is the optimal order.

4 Numerical experiments

The goal of this paper is to perform systematic numerical experiments in order to understand the dependence of the coarsest mesh width on various parameters and to get insights in the sharpness of theoretical predictions. We consider the following model problem. Let $\Omega \subset \mathbb{R}^d$ denote a bounded domain and let $a : H_0^1(\Omega) \times H_0^1(\Omega) \to \mathbb{R}$ be the bilinear form

$$a(u, v) := \int_\Omega \langle \mathbf{A}(x) \nabla u, \nabla v \rangle + cuv,$$

where $\mathbf{A} \in \mathbf{L}^\infty(\Omega, \mathbb{R}^{d \times d})$ is symmetric and uniformly positive definite. The coefficient c is a bounded $L^\infty(\Omega, \mathbb{R})$ function.

For $\inf_{x \in \Omega} c(x) \geq 0$, the distribution of eigenvalues, asymptotically, is described by [cf. (3.1)]

$$\frac{\delta(\lambda)}{\lambda} \approx C \lambda^{-d/2} \tag{4.1}$$

(see [26], [9, Sects. VI, 4, Satz 17 and 19], [4,5], [19, Theorem 13.1]). If an eigenvalue λ satisfies (4.1) we conclude from [22, Corollary 2.17 and 2.19] that, for piecewise linear finite elements, the condition

$$\lambda^{\frac{d+1}{2}} h_0 \lesssim 1 \tag{4.2}$$

on the coarsest mesh h_0 width guarantees that

a. the eigenvalue approximations satisfies

$$\frac{|\lambda - \lambda_S|}{\lambda} \lesssim \lambda h^2 \quad \forall 0 < h \leq h_0 \tag{4.3}$$

b. the eigenvector approximations satisfy

$$\|e - e_S\|_{H^1(\Omega)} \lesssim \left(1 + \lambda^{\frac{2+d}{2}} h\right) \sqrt{\lambda} h$$
$$= \sqrt{\lambda} h + \lambda^{\frac{3+d}{2}} h^2 \overset{(4.2)}{\lesssim} \sqrt{\lambda} h \tag{4.4}$$

for all $0 < h \leq h_0$.

Paper [22] does not contain estimates for the eigenvalue multigrid method and one goal of the following numerical experiments is to give insights on the coarsest possible mesh width also for the multigrid method.

4.1 Tests in one dimension

As in [11], we have considered the Mattieu equation, where $\Omega = (0, \pi)$, $\mathbf{A} = 1$, and $c(x) = 20 \cos(2x)$. Table 1 lists the maximal step size h_0 so that the asymptotic convergence rates become visible. In Fig. 1 we have depicted exemplarily the convergence history for the 21st eigenvalue and -function as a function of $h \to 0$. We observe that the maximal mesh sizes as shown in Table 1 are the limiting values for the asymptotic convergence rates of *all* three quantities:

- the eigenvalues,
- the H^1-errors of the eigenfunctions,
- and the L^2-errors.

Table 1 clearly shows, that condition (4.2) is too strict for this model example and the weakened condition

$$h \sqrt{|\lambda|} \lesssim 1 \tag{4.5}$$

Table 1 Maximal step size h_0 so that the quadratic convergence holds for all $h \leq h_0$

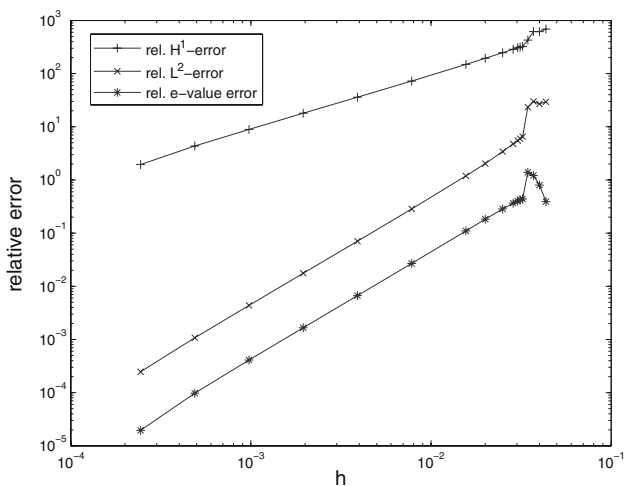| λ	−13.9	−2.4	8.0	17.4	26.8	37.4	50.0	64.8
h_0	1/7	1/7	1/7	1/10	1/10	1/10	1/11	1/13
$\sqrt{|\lambda|}h_0$	0.5	0.2	0.4	0.4	0.5	0.6	0.6	0.6
λ	81.6	100.5	121.4	144.4	169.3	196.2	225.2	256.2
h_0	1/15	1/15	1/17	1/18	1/19	1/21	1/23	1/23
$\sqrt{\lambda}h_0$	0.6	0.7	0.6	0.7	0.7	0.7	0.7	0.7
λ	289.2	324.2	361.1	400.1	441.1	484.1	529.1	576.1
h_0	1/25	1/27	1/28	1/30	1/32	1/34	1/35	1/37
$\sqrt{\lambda}h_0$	0.7	0.7	0.7	0.7	0.7	0.6	0.7	0.6

Fig. 1 Convergence of the relative $H^1(\Omega)$- and $L^2(\Omega)$-errors and the relative eigenvalue error as a function of h for the 21st eigenfunction and -value. The figure is drawn in a log–log scale

is sufficient.

By using the condition as in Table 1 the quadratic convergence of the eigenvalues starts for $h \leq h_0$.

Remark 4.1 The relaxed stability condition (4.5) compared to the theoretical bound (4.2) might be explained by [22, Example 4.5]: In one dimension (for the Laplace eigenvalue problem), the discrete eigenfunctions are the interpolants of the exact eigenfunctions and one can derive the relaxed condition (4.5) for this special case. Although, for the Mattieu problem, the Galerkin finite element solution differs from the interpolant, the difference is quite small and a similar effect as in [22, Example 4.5] might be the reason for the observed behavior.

In order to verify the eigenvalue error estimate (4.3) we have computed the quantity

$$E_1(\lambda) := \frac{|\lambda - \lambda_S|}{(\lambda h)^2} \quad \text{with} \quad h = h_0/2 \quad \text{and} \quad h_0 \text{ as in Table 1}.$$

In Table 2, we have listed $E_1(\lambda)$ which clearly shows that for the chosen example the estimate is sharp.

In the next experiment, we have investigated the relative H^1-error of the eigenfunctions. We have chosen the mesh size so that $\sqrt{|\lambda|}h = 1/10$. Then, the theoretical error estimate (4.4) takes the form

$$\|e - e_S\|_{H^1(\Omega)} \leq C\left(1 + |\lambda|^s\right) \quad \text{with} \quad s = 1. \quad (4.6)$$

The numerical experiment is performed to see whether the power $s = 1$ in (4.6) is sharp. We have plotted the function

$$E_2(\log \lambda) := \log \|e - e_S\|_{H^1(\Omega)}, \quad \text{where} \quad h = \frac{1}{10\sqrt{|\lambda|}}$$

in Fig. 2, where—as comparison—the line $g(x) = x - 5/2$ is also depicted. We deduce that $s = 1$ holds and the theoretical bound is sharp.

Finally, we have investigated the coarsest possible mesh width for the eigenvalue multigrid method. We have chosen a two-grid method (which is the most critical case for the eigenvalue multigrid) and the maximal step size h_0 for the coarse mesh such that the averaged convergence rates κ are at most 0.7. From Table 3 we conclude that, for this model problem, the condition $\sqrt{|\lambda|}h_0 \lesssim 1$ for the coarsest mesh

Table 2 Ratio $E_1(\lambda)$ for different values of λ and h_0 chosen as in Table 1

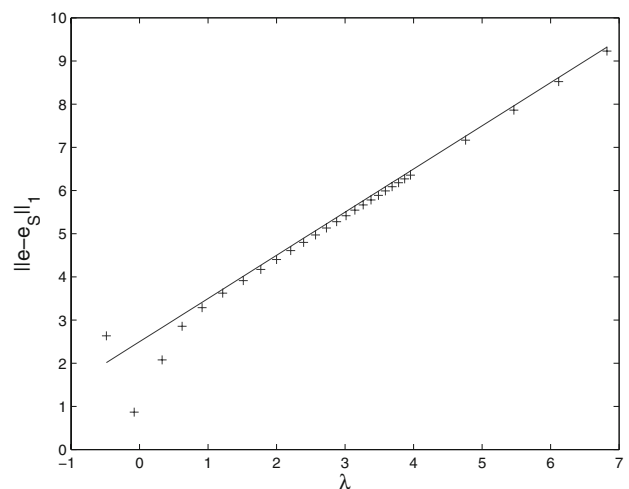| λ	−13.9	−2.4	8.0	17.4	26.8	37.4	50.0	64.8
$E_1(\lambda)$	0.1	15.8	3.0	1.1	0.8	0.8	0.8	0.8
λ	81.6	100.5	121.4	144.4	169.3	196.2	225.2	256.2
$E_1(\lambda)$	0.8	0.8	0.8	0.8	0.8	0.8	0.8	0.8
λ	289.2	324.2	361.1	400.1	441.1	484.1	529.1	576.1
$E_1(\lambda)$	0.8	0.8	0.8	0.8	0.8	0.8	0.8	0.8

Fig. 2 The relative H^1-error as a function of λ is shown. The comparison with a line of slope 1 shows that the theoretical value $s = 1$ in (4.6) turns out to be sharp for this example

Table 3 Maximal coarse mesh width h_0 so that the eigenvalue two-grid method converges

λ	-13.9	-2.4	8.0	17.4	26.8	37.4	50.0	64.8
h_0	1/6	1/6	1/6	1/6	1/6	1/7	1/7	1/9
$\sqrt{\lvert\lambda\rvert}h_0$	0.6	0.3	0.5	0.7	0.9	0.9	1.0	0.9
κ	0.27	0.25	0.28	0.5	0.43	0.48	0.53	0.57
λ	81.6	100.5	121.4	144.4	169.3	196.2	225.2	256.2
h_0	1/11	1/12	1/12	1/13	1/14	1/18	1/19	1/20
$\sqrt{\lambda}h_0$	0.8	0.8	0.9	0.9	0.9	0.8	0.8	0.8
κ	0.6	0.7	0.66	0.68	0.7	0.65	0.66	0.68
λ	289.2	324.2	361.1	400.1	441.1	484.1	529.1	576.1
h_0	1/21	1/23	1/24	1/26	1/27	1/28	1/30	1/31
$\sqrt{\lambda}h_0$	0.8	0.8	0.8	0.8	0.8	0.8	0.8	0.8
κ	0.69	0.66	0.67	0.66	0.67	0.69	0.67	0.69

width is sufficient for the convergence of the eigenvalue multigrid method.

4.2 Experiments in two dimensions

In two dimensions we consider the case $\Omega = (0, 1) \times (0, 2)$, $\mathbf{A} = \mathbf{I}$ the identity, and $c \equiv 0$, i.e., we consider the Dirichlet Laplacian on the rectangle Ω.

4.2.1 Convergence of the eigenfunctions

The first set of experiments concerns the convergence of the eigenfunctions, i.e., the investigation of the error $\|e - e_S\|_{H^1(\Omega)}$. In Fig. 3, the relative H^1-error of some eigenfunctions as a function of the mesh width is depicted and the following observations can be made.
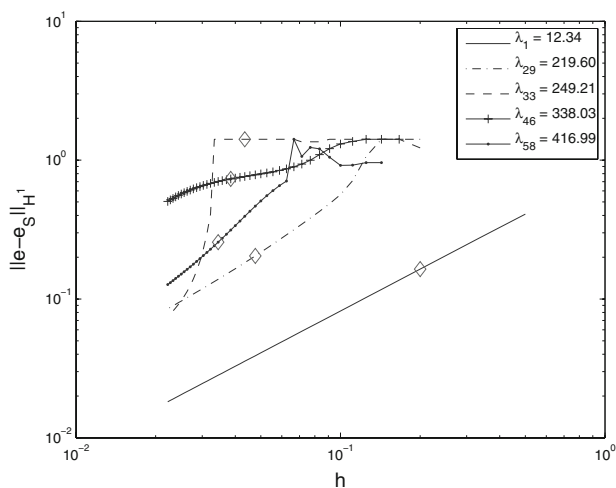

Fig. 3 The convergence of the error $\|e - e_S\|_{H^1(\Omega)}$ against the decreasing mesh width h. The results are shown for λ_1, λ_{13}, λ_{20}, λ_{33}, and λ_{59} on a log–log scale. We also highlight the errors for the choice $h\sqrt{\lambda} \approx 0.7$

1. The relative error stays at 100% until a threshold h_0 is reached. Then, a transition region is passed through, where the *pollution* term $\lambda^{\frac{2+d}{2}}h$ in (4.4) becomes negligible before, finally, the asymptotic convergence rate $\sqrt{\lambda}h$ is reached.

2. In contrast to the one-dimensional example, the relaxed condition (4.5) is not sufficient to guarantee that the error starts to decrease for all $h \le h_0$. For all examples, the theoretical condition (4.2) was sufficient so that the asymptotic convergence rate holds for $h \le h_0$.

3. The maximal step size h_0 decreases with larger values of λ. Interestingly, this decrease is not monotonic. This behavior could be explained by considering the eigenvalues $\lambda_{n,m} := \pi^2 \left(n^2 + m^2/4\right)$ of the continuous Laplacian on $(0, 1) \times (0, 2)$. A minimal condition for the relative finite element error for an eigenfunction corresponding to some $\lambda_{n,m}$ to be smaller than 100% is given by

$$h_0 \max\left\{n, \frac{m}{2}\right\} = c \quad \text{for some } c \lesssim 1, \tag{4.7}$$

i.e., the oscillations of the wave are resolved by – at least – a few mesh points. Consider two eigenvalues $\lambda_{n,1} \le \lambda_{\tilde{n},\tilde{\nu}}$ with $\tilde{n} = \lceil n/\sqrt{2} \rceil$ and $\tilde{\nu} = \lceil \sqrt{2}n \rceil$, where $\lceil x \rceil$ denotes the smallest integer which is larger than or equal to x. For the eigenvalue $\lambda_{n,1}$, condition (4.7) is more restrictive than for the larger eigenvalue $\lambda_{\tilde{n},\tilde{\nu}}$. This observation, possibly, explains why the restriction on the coarsest mesh width may not be always *monotonously* decreasing with increasing eigenvalue.

The eigenvalues for the Laplacian on the rectangle $(0, 1) \times (0, 2)$ are not uniformly distributed. We have avoided to compute multiple eigenvalues because our multigrid implementation is designed only for single eigenvalues and, in addition, the pre-asymptotic convergence theory in [22] does not cover this case. However, the remaining eigenvalues which we have considered are far from obeying the asymptotic distribution law. Hence, we also investigate the behavior in the error $\|e - e_S\|_{H^1(\Omega)}$ in dependence of λ and $\delta(\lambda)$ (cf. (3.1)) when $\sqrt{\lambda}h \approx 2/3$. The results are given in Fig. 4 where we compared $\|e - e_S\|_{H^1(\Omega)}$ with $\lambda/\delta(\lambda)$.

4. Estimate (4.4) is obtained by inserting the asymptotic distribution law (4.1) into (cf. [22, (4.15)])

$$\|e - e_S\|_{H^1(\Omega)} \lesssim \left(1 + \frac{\lambda^2}{\delta(\lambda)}h\right)\sqrt{\lambda}h.$$

Since $\sqrt{\lambda}h = 2/3$ is fixed we get

$$\|e - e_S\|_{H^1(\Omega)} \lesssim 1 + \frac{\lambda^s}{\delta(\lambda)} \quad \text{with} \quad s = 3/2. \tag{4.8}$$
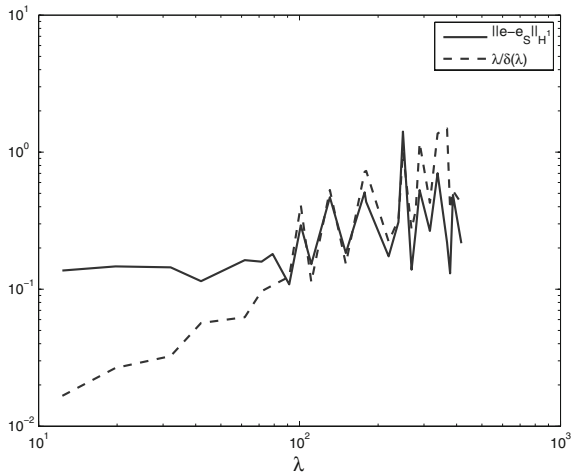
Fig. 4 We plot $\|e - e_S\|_{H^1(\Omega)}$ against λ for $\sqrt{\lambda}h \approx 2/3$. We compare this with $\lambda/\delta(\lambda)$

Figure 4 shows that the functions $\|e - e_S\|_{H^1(\Omega)}$ and $\lambda/\delta(\lambda)$ have the same qualitative behavior. There are too few experimental values in order to verify whether the power $s = 3/2$ in (4.8) is sharp or whether a smaller value s (e.g., $s = 1$) is fitting the error function better. However, it is clearly visible that the factor of $\delta(\lambda)^{-1}$ in (4.8) is sharp for the considered example.

4.2.2 Convergence of the eigenvalues

We next investigate the convergence of eigenvalues and, as in the one-dimensional case, find the condition (4.2) to be too strict. In Fig. 5 we plot the behavior of $|\lambda_S - \lambda|/\lambda^2$. We see that most eigenvalues (including the higher ones) of the finite element system matrix are already—at least—stable
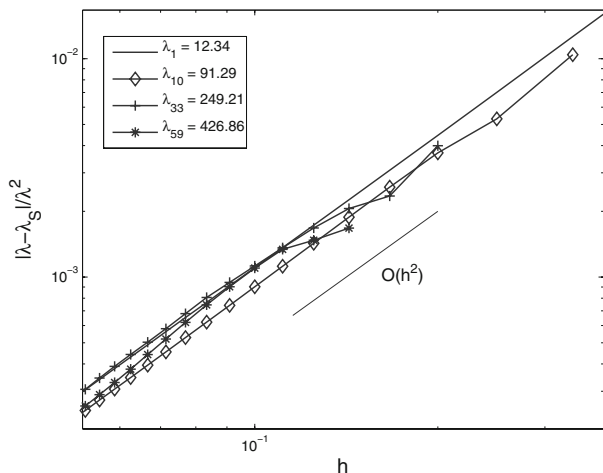
approximations to some exact eigenvalue. More precisely, if we denote the spectrum of the discrete problem (2.4) corresponding to the mesh $\mathcal{G}_\ell$ and the finite element space S_ℓ by σ_ℓ and order the eigenvalues increasingly (by taking into account their multiplicity), i.e.,

$$0 < \lambda_{\ell,1} \le \lambda_{\ell,2} \le \ldots \lambda_{\ell,N_\ell}$$

then, the following observation can be read off Fig. 5: there exist some constants $c \in (0, 1)$ and $C > 0$ independent of ℓ such that

$$\frac{|\lambda_{\ell,j} - \lambda_j|}{\lambda_j^2} \le Ch_\ell^2 \quad \forall 1 \le j \le cN_\ell, \tag{4.9}$$

where $N_\ell = \dim S_\ell$ and λ_j denotes the jth exact eigenvalue. Thus, (4.9) clearly shows the quadratic convergence of the eigenvalues.

The fact that most discrete eigenvalues of a finite element discretization are already—at least—stable approximations to some exact eigenvalues, is, at first glance, surprising because the convergence of the corresponding eigen*functions* has not started for the higher eigenvalues if j in (4.9) is large, i.e., $j \sim cN_\ell$, and λ is large. An explanation, possibly, is that the eigenvalues are *integrated* quantities of the eigenfunctions (via the Rayleigh quotient) and, although, the accuracy of an eigenfunction with respect to the H^1-norm is poor it contains already enough accurate information for the determination of a good approximation of the eigenvalue. Figures 6 and 7 clearly support this explanation: In the range of h, where the relative H^1-error of the eigenfunction corresponding to λ_{33} still is 100%, the relative error for the eigenvalue is already properly decreasing with the asymptotic rate. The plot of the eigenfunctions in Fig. 7 gives more insights in the behavior of the approximate eigenfunctions as
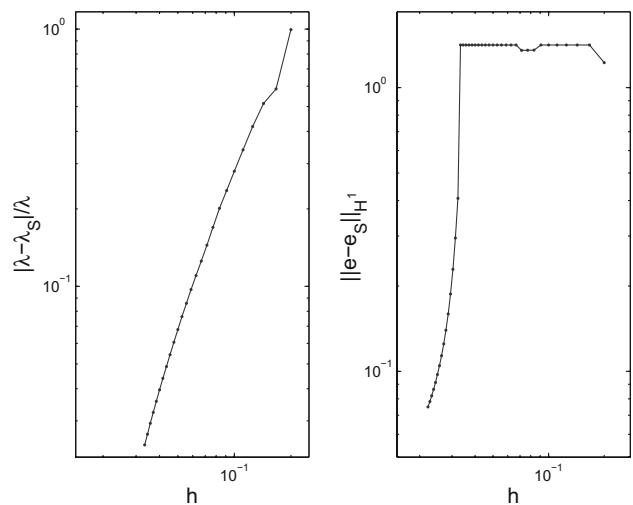

Fig. 5 The convergence of the error $|\lambda_S - \lambda|/(\lambda^2)$ against the decreasing mesh width h. The results are shown for λ_1, λ_{10}, λ_{33}, and λ_{59}

Fig. 6 The convergence of the relative errors $|\lambda_S - \lambda|/\lambda$ and $\|e - e_S\|_{H^1(\Omega)}$ against the decreasing mesh width h. The results are shown for λ_{33}
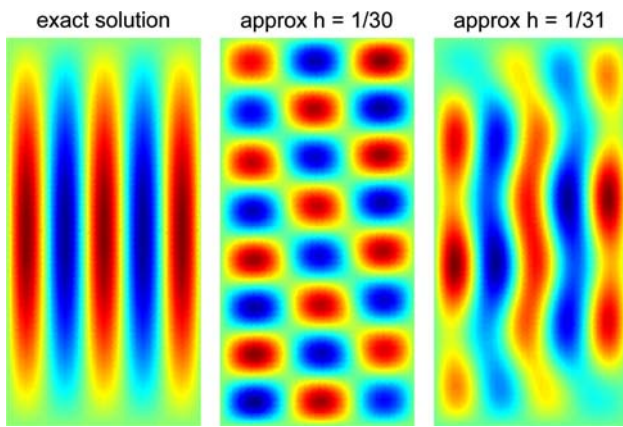
Fig. 7 The exact eigenfunction with eigenvalue λ_{33} and two approximations for $h = 1/30$ and $h = 1/31$. For $h = 1/30$ the approximation is in fact approximate eigenfunction for the repeated eigenvalue $\lambda_{31} = \lambda_{32}$

the mesh width tends to zero. Let $\left(\lambda_{h,j}, e_{h,j}\right)$ denote the jth eigenpair (counted increasingly and taking into account the multiplicity) for the finite element discretization with step width h. Then, for $\tilde{h} = 1/30$, Fig. 7 shows the exact eigenfunction and, in the middle, the eigenfunction $e_{\tilde{h},33}$. It turns out that $e_{\tilde{h},33}$ is much closer to the exact eigenfunction e_{32} than to e_{33} and, consequently, the H^1-error is 100% as can be seen in the right picture of Fig. 6. Although $\lambda_{\tilde{h},33}$ might also be considered as an approximation of λ_{32} the comparison with λ_{33} gives also a relative error below 100%. The reason is that the relative difference of two subsequent eigenvalues is, asymptotically, tending to zero as can be seen from (4.1)

$$\frac{\left|\lambda_{j+1} - \lambda_j\right|}{\lambda_j} \lesssim C\lambda_j^{-d/2} \overset{j\to\infty}{\to} 0.$$

4.2.3 Multigrid convergence

One essential ingredient for the multigrid convergence is related to the accuracy of the approximations of the eigenfunctions on coarse grids $\mathcal{G}_\ell$ which should already exhibit the asymptotic convergence with respect to the coarse mesh width h_ℓ. Hence, we expect that the condition on the coarsest mesh width in the multigrid algorithm is in analogy to the condition for the approximation of the eigenfunctions.

In Table 4, among other results, we show the maximal mesh width such that the multigrid iteration converges efficiently.

For the 33rd eigenfunction even for $h_0 = 1/35$ we have not obtained a rate of convergence for the multigrid method which is smaller than 0.3. The non-monotonic decrease of the coarsest mesh width, possibly, can be explained as the third observation in Sect. 4.2.1.

Table 4 The results are only for the simple eigenvalues of the rectangle $(0, 1) \times (0, 2)$

j	λ_j	$1/h_0$	$\sqrt{\lambda_j}h_0$	$E_1(\lambda_j)$	$1/h_{MG}$	Rate
1	12.337	5	0.7	0.08	2	0.2
2	19.739	6	0.7	0.09	3	0.3
3	32.076	8	0.7	0.09	4	0.3
4	41.946	9	0.7	0.08	6	0.3
7	61.685	11	0.7	0.1	6	0.3
8	71.555	12	0.7	0.09	10	0.3
9	78.957	12	0.7	0.1	8	0.3
10	91.294	13	0.7	0.08	12	0.3
13	101.163	14	0.7	0.1	17	0.3
14	111.033	15	0.7	0.1	13	0.2
17	130.772	16	0.7	0.1	16	0.3
18	150.511	17	0.7	0.1	16	0.3
23	177.653	19	0.7	0.1	20	0.3
24	180.120	19	0.7	0.1	20	0.2
29	219.599	21	0.7	0.1	20	0.2
30	239.338	21	0.7	0.09	26	0.3
33	249.208	22	0.7	0.09	–/–	–/–
36	268.947	23	0.7	0.09	26	0.3
37	278.816	23	0.7	0.1	35	0.4
40	288.686	24	0.7	0.1	–/–	–/–
43	315.827	25	0.7	0.1	35	0.2
46	338.034	26	0.7	0.1	–/–	–/–
51	367.643	27	0.7	0.1	–/–	–/–
52	377.512	27	0.7	0.09	–/–	–/–
53	387.382	27	0.7	0.09	35	0.3
58	416.991	28	0.7	0.1	35	0.2
59	426.860	29	0.7	0.08	35	0.3

Given are h_0 so that $\sqrt{\lambda_k}h_0 \approx 0.7$ and the error $E_1(\lambda_j)$ for this choice of meshwidth. Next h_{MG} is the largest meshwidth so that the multigrid method converges with a rate smaller than or equal to 0.3

References

1. Babuška, I., Aziz, A.K.: The mathematical foundation of the finite element method. In: Aziz, A.K. (ed.) The Mathematical Foundation of the Finite Element Method with Applications to Partial Differential Equations, pp. 5–359. Academic Press, New York (1972)
2. Babuška, I., Osborn, J.: Eigenvalue problems. In: Ciarlet, P., Lions J. (eds.) Finite Element Methods (Part 1). Handbook of Numerical Analysis, vol. II, pp 641–788. Elsevier Science Publishers, Amsterdam (1991)
3. Brandt, A., McCormick, S., Ruge, J.: Multigrid methods for differential eigenproblems. SIAM J. Sci. Stat. Comput. **4**, 244–260 (1983)
4. Brownell, F.: Extended asymptotic eigenvalue distributions for bounded domains in n-space. Pac. J. Math. **5**, 483–499 (1955)
5. Brownell, F.: An extension of Weyl's asymptotic law for eigenvalues. Pac. J. Math. **5**, 483–499 (1955)
6. Cai, Z., Mandel, J., McCormick, S.: Multigrid methods for nearly singular linear equations and eigenvalue problems. SIAM J. Numer. Anal. **34**, 178–200 (1997)

7. Chatelin, F.: La méthode de Galerkin. Ordre de convergence des éléments propres. C.R. Acad. Sci. Pairs Sér. A **278**, 1213–1215 (1974)

8. Chatelin, F.: Spectral Approximation of Linear Operators. Academic Press, New York (1983)

9. Courant, R., Hilbert, D.: Methoden der Mathematischen Physik. Bd. 1. Springer, Berlin (1924)

10. Friese, T., Deuflhard, P., Schmidt, F.: A multigrid method for the complex Helmholtz eigenvalue problem. In: Lai, C.-H., Bjorstad, P., Cross, M., Widlund, O. (eds.) Procs. 11th International Conference on Domain Decomposition Methods, pp. 18–26. DDM-org Press, Bergen (1999)

11. Hackbusch, W.: On the computation of approximate eigenvalues and eigenfunctions of elliptic operators by means of a multi-grid method. SIAM J. Numer. Anal. **16**(2), 201–215 (1979)

12. Hackbusch, W.: Multi-Grid Methods and Applications, 2nd edn (2003). Springer, Berlin (1985)

13. Hackbusch, W.: Elliptic Differential Equations. Springer, Heidelberg (1992)

14. Heuveline, V., Bertsch, C.: On multigrid methods for the eigenvalue computation of nonselfadjoint elliptic operators. East West J. Numer. Math. **8**, 275–297 (2000)

15. Hwang, T., Parsons, I.: A multigrid method for the generalized symmetric eigenvalue problem: Part I algorithm and implementation. Int. J. Numer. Meth. Eng. **35**, 1663 (1992)

16. Hwang, T., Parsons, I.: A multigrid method for the generalized symmetric eigenvalue problem: Part II performance evaluation. Int. J. Numer. Meth. Eng. **35**, 1677 (1992)

17. Hwang, T., Parsons, I.: Multigrid solution procedures for structural dynamics eigenvalue problems. Comput. Mech. **10**, 247 (1992)

18. Knyazev, A., Neymeyr, K.: Efficient solution of symmetric eigenvalue problems using multigrid preconditioners in the locally optimal block conjugate gradient method. Electron. Trans. Numer. Anal. (ETNA) **15**, 38–55 (2003)

19. Levendorskii, S.: Asymptotic Distribution of Eigenvalues of Differential Operators. Springer, Berlin (1990)

20. Livshits, I.: An algebraic multigrid wave-ray algorithm to solve eigenvalue problems for the Helmholtz operator. Numer. Linear Algebra Appl. **11**(4), 229–339 (2004)

21. Livshits, I., Brandt, A.: Accuracy properties of the wave-ray multigrid algorithm for Helmholtz equations. SIAM J. Sci. Comput. **28**(4), 1228–1251 (2006)

22. Sauter, S.: Finite Elements for Elliptic Eigenvalue Problems in the Preasymptotic Regime. Technical Report, Math. Inst., Univ. Zürich, 17, 2007

23. Sauter, S.A., Wittum, G.: A multigrid method for the computation of eigenmodes of closed water basins. Impact Comput. Sci. Eng. **4**, 124–152 (1992)

24. Schmidt, F., Friese, T., Zschiedrich, L., Deuflhard, P.: Adaptive multigrid methods for the vectorial maxwell eigenvalue problem for optical waveguide design. In: Jäger, W., Krebs, H.-J. (eds.) Mathematics. Key Technology for the Future, pp. 279–292. Springer, Heidelberg (2003)

25. Strang, G., Fix, G.: An Analysis of the Finite Element Method. Prentice-Hall, Englewood Cliffs (1973)

26. Weyl, H.: Das asymptotische Verteilungsgesetz der Eigenwerte linearer partieller Differentialgleichungen (mit einer Anwendung auf die Theorie der Hohlraumstrahlung). Math. Ann. **71**, 441–479 (1912)